IOSR Journal of Applied Physics (IOSR-JAP)
e-ISSN: 2278-4861.Volume 8, Issue 6 Ver. III (Nov. - Dec. 2016), PP 54-59
www.iosrjournals.org

Evidence of half-metallic behaviour for $FeFe_2O_4$

A. Elfalaky[a], S. Soliman[a] and H.Elmosallamy[a]
[(a)]*Zagazig University, Faculty of Science, Department of Physics, Zagazig, Egypt.*

Abstract: *The electronic structure and magnetic properties of Fe_3O_4 have been studied by density functional method in the frame of local density approximation. Gradually reducing the symmetry has been used to establish different cation distribution of the studied compound. This symmetry cracking introduces some evidences for the half-metallicity of Fe_3O_4. Different experimental distributions, of cations Fe^{+2} and Fe^{+3} between tetrahedral A-site and octahedral B-site for spinel structure, have been calculated. The magnetic anisotropy through the spin-orbit coupling (SOC) has been calculated, where the results revealed a pronounced agreement with the experimental results. These SOC calculations have been conducted for different directions of the magnetization, where semiconductor and metallic behavior for majority and minority channels, respectively, are still found respectively. As for Fe in B-site, the spin orbital angular momentum coupling component of the magnetic momentis considerably larger than that for Fe in A-site. This urges some states of Fe-3d electrons on B-siteto have higher energy states than the Fermi energy.*

I. Introduction

Ferrites are interesting magnetic materials from the academic point of view, additionally, ferrites are involved in high frequency applications like antennae and various microwave. This is because large number of these materials can be prepared as insulating ferromagnet at room temperature [1–7]. Ferrites properties can be adjusted and strongly changed according to many parameters and conditions such as methodology used in synthesis, heat treatment, constituents and structure [3, 5–11]. To have better understanding for the physical properties of any material and ferrite in particular, the crystal structure of the material should be clearly identified. In ferrite, the structure has significant influence on the magnetic, electrical and dielectric properties. Ferrite has a Centrosymmetric cubic structure named spinel structure in which the cations are arranged in two sublattices named A-site and B-site. Most of the ferrite properties, and hence application, depend solely on the cation distribution among these sublattices. In normal spinel, A-side, with tetrahedral shape, contains the divalent ions, and B-side, with octahedral shape, includes the trivalent ions. In the mixed spinel structure, a ratio of divalent and trivalent cations can occupy the B-side and A-side respectively. In the inverse spinel, A-site and B-site are totally filled with the trivalent and divalent respectively [12, 13].

Ferrites have the formula AFe_2O_4 where A is a metal atom and mostly a transition metal atom. This formula indicates that, ferrites have partially filled 3d shells. This means that the conduction and valance bands are overlapping, so ferrite should behave as a conductor.Conversely most of ferrites have an insulating behavior with very small gap from 0.04 to 0.06 eV [14–18]. Long ago, the main explanation for the electrical properties of ferrites was governed by the electronic exchange interaction between these two sites as formulated in the Goodenough-Kanamorirule [10, 12]. The electronic structure calculations have indicated some new explanations for the insulating behavior depending on the expansion or contraction of the A and B sites, because of the deviation of the oxygen positional parameter. Additionally density functional theory (DFT) calculations for some ferrites have shown that the 3d states are low lying states from Fermi level [9, 13]. Previous studies have shown that magnetite Fe_3O_4 is a spinel type structure with an inverse-spinel ratio [8, 14]. Recently it has been proposed that, magnetite is described with $Fe^{+2.5}$ in the octahedral site at ambient conditions to make the electron delocalization more obvious [19].

When magnetite is heated to just above 122K, a threshold temperature called the Verwey temperature, conductivity increases to more than two orders of magnitude [19]. Above 120K, half of the Fe^{+3} moments are lined in parallel with Fe^{+2} magnetic moments, but the remaining Fe^{+3} magnetic moments are in the opposite direction leading to a decrease in the magnetic moment as in the form $(Fe^{+2}\ Fe^{+3})[Fe^{+2}\ 3Fe^{+3}]O_8$ [15, 17]. The present Spin-Orbit Coupling calculations have been done so as to draw a minute picture of the electric and magnetic properties for Fe_3O_4. Calculate the deviation of Oxygen-parameter from the ideal value. Pin- pointing precisely the stable spin states for the compound. Additional features in the magnetization reversal behavior have also been spotlighted by breaking the symmetry. This urges nonsymmetrical reversal behavior around the easy axes in the magnetic crystal. The distortion of the local lattices structure of Fe^{+3} and Fe^{+2}ions located at the octahedral site and tetrahedral site respectively has been studied. The on-site exchange is also taken into consideration as it is very useful for strongly correlated systems enabling to see the behavior of the studied compound.

II. Crystal Structure And Calculation Details

The physical properties of solid depend mainly on the local configuration of the atoms or ions composed of it. There are two important types of oxygen interstices, 64 having fourfold coordination, of which 8 (A-sites or tetrahedral-sites) may be occupied by divalent cations, and 32 having sixfold coordination, of which 16 (B-sites or octahedral-sites) may be occupied by the trivalent cations. The site symmetries and overall symmetry are expressed by the crystallographic space group Fd−3m. More about the spinel structure is discussed in details in ref [7]. The cations are in special positions determined by symmetry, and the structure is centrosymmetrical about the B-site. The conventional choices for the unit cell origin in spinel are either $\bar{4}$3m on an A-site cation or $\bar{3}$m on an octahedral vacancy. The anion positions are specified in details in terms of a single positional parameter u which has the value 3/8 for origin $\bar{4}$3m or 1/4 for origin $\bar{3}$m for an ideal spinel [1]. In practice, u is often found to be larger than the ideal value. When u is greater than 3/8 or 1/4, the anion moves in [111] direction outwards from the nearest A-site. This makes the study of the u-deviation, which leads to the breaking of symmetry, more urgent. The calculated structure parameters for the normal spinel Fe-ferrite with space group 227(Fd−3m) have been used for the electronic structure calculations. The optimized lattice parameter is 8.41°A which is likely the same as the experimental value [20]. The spinel properties are sensitive to the oxygen-structure parameter.So optimization has been carried out to get a reasonable value for the oxygen positional u parameter [12]. Our calculated value of u was found to be 0.255 which is in a close agreement with the experimental value [14]. The Spin-Orbit coupling calculations based on density functional theory has been performed using Local augmented plane wave (LAPW) code Wien2k [21, 22]. Local orbitals have been employed for treating the high lying semicore states of Fe-3d and to minimize the linearization errors. Exchange correlation has been taken within the generalized gradient approximation GGA in the parameterization by Perdew et al [23]. The energy threshold between the core and the valance states has been set at -6.8Ry. The muffin tin-radii (R_{MT}) of Fe=1.89 and O =1.67 °A have been chosen to ensure that the spheres nearly touch one another and to minimize the interstitial space. To reach a convergence for the basis of the wave function, the cut of parameter R_{MT} K_{MAX} = 7 has been taken for the number of plane waves. The expansion of the partial wave functions has been set to L=10 inside the muffin tin atomic spheres while the charge density has been Fourier expanded up to G = 12. In self-consistent calculations, a grid of 5000 k-points has been employed in the irreducible Brillouin zone resulting in 173 mesh with 405 point. The energy and charge convergence criterions have been set to 10^{-4} Ry and 10^{-3} e respectively. The convergence criteria for atomic forces is set to 10^{-3} Ry/au.

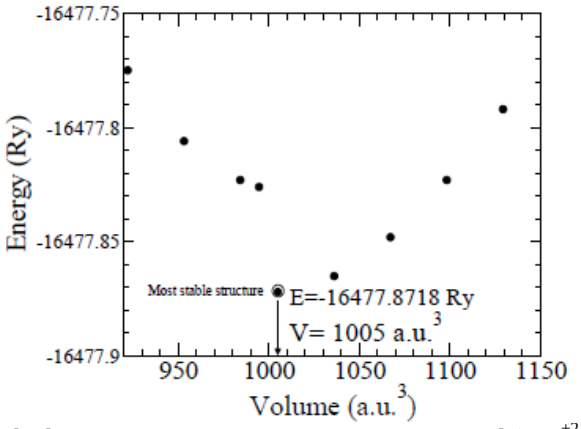

FIG. 1. Full optimization for the lowest energy spin arrangement compound $(2Fe^{+2})[4Fe^{+3}]O_8$ with space groups 227 (Fd-3m), in table one.

III. Results And Discussion

Structural optimization by adjusting the spin alignment, oxygen position parameter u and latice constant a have been considered. Once the minimum energy is achieved, the density of states, charge distribution and band structure will be inspected.

A. Optimization

In spinel, as u increases above the ideal value, anions move away from the tetrahedral coordinated A-site cations along the [111] directions. This in turn will increase the volume of A-site interstices while the octahedral B-site which is smaller than A-site will become correspondingly more smaller. Thus, for the given spinel compound, the anion sublattices A and B expand or constrict by u-change, until the A- and B-site volumes match the radii of the constituent cations. The calculated value for the oxygen positional parameter is 0.255 with a deviation of 0.05 from the ideal value. Hence the symmetry of the regular tetrahedral of A-site is

unchanged by the anion-lattice dilation, but B-site will suffer from symmetry reduction. Such distortion of the octahedral symmetry has been recorded experimentally for $MgAl_2O_4$ and other spinels [4, 24]. This change in symmetry may produce a new point group for Fe^{+2} and Fe^{+3} in A and B-sites respectively. Consequently, the spinel space group 227 (Fd−3m) may be changed [4, 24]. Full optimization for Fe_3O_4 is shown in figure 1. This optimization is based on the calculated forces on the atoms. These atoms follow the symmetry constraints of a certain space group. Where updating of atom positions occurs for the lowest force on atoms per formula unit. From that updating of atom positions, the free structure oxygen positional parameter will be determined.

B. DOS Calculations

Crystal field splitting in transition metal oxides are mainly the result of hybridization between oxygen 2p levels and metal d states of transition metal (TM). This crystal field urges some d-states for TM to be in energy higher than Fermi energy which in turn produces the half metallicity for the spinel with normal frame work methods of calculations [25].

Figure 2 shows a half-metallic ferrimagnetic material with a conductive minority spin channel and semi conductive majority spin channel. Additional calculations, to overcome the half-metallicity, have been carried out by GGA+U with U=7 eV as shown in figure 2 where U is the Hubbard parameter. Figure 2 shows that, theapplicationof Utends to move the occupied states away from Fermi level and that does not destroy the half metallicity as expected in [26, 27]. This is in contrast to the predicted semiconductor behavior in ref [28]. The majority gap between occupied Fe^{+3}3d states in B-site and empty Fe^{+2}3d in A-site is still noticed and it does not disappear by U=7 eV. Worthy mentioned, there are some published theoretical results about the insulating behavior with a U-value lower than 7 eV resulting in a large gap [18, 28]. But it is well known that, ferrites behave as small-gap, semiconductor, not more 0.2 eV, and as insulators at low temperatures [29].

For minority channel in octahedral symmetry, the d-orbitals split into two sets with an energy difference oct (the crystal-field splitting parameter). The first set is d_{xy}, d_{xz} and d_{yz} orbitals at a low energy while the second one is d_z^2 and $d_{x^2-y^2}$at a high energy. The three lower energy orbitals are collectively referred to as t_{2g}, and the two higher-energy orbitals as e_g. These labels are based on the theory of molecular symmetry. Figure 6 shows an overlapping between occupied t_{2g} and empty e_g around Fermi level which is the reason for the metallic behavior for minority channel. The crystal field is known to be in opposite direction to the minority states which in turn force eg to lower energy until over- lapping occurs between e_g and t_{2g} around Fermi energy. This is the reason for the theoretical half metallicity of spinel. It is experimentally known that the $FeFe_2O_4$ has semiconducting properties [28].

The challenge now is to overcome the overlapping of e_g and t_{2g} for minority channel in spinel gap 0.2 eV. The DOS calculations have been carried out with values higher and lower than the optimized u-value 0.255 as an initial testing. The usedvalues are u=0.245, 0.25 and 0.26.Such an increase and decrease in u value has no significant effect on the DOS. I. Leonov et al. indicated that at room temperature, magnetite crystallizes in the inverted cubic spinel structure Fd-3m with tetrahedral A-sites occupied by Fe^{+3} cations, whereas octahedral B-sites occupied by an equal number of randomly distributed Fe^{+2} and Fe^{+3} cations [18, 25]. The DOS calculations have been carried out using I. Leonov0s configurations as shown in table 1.

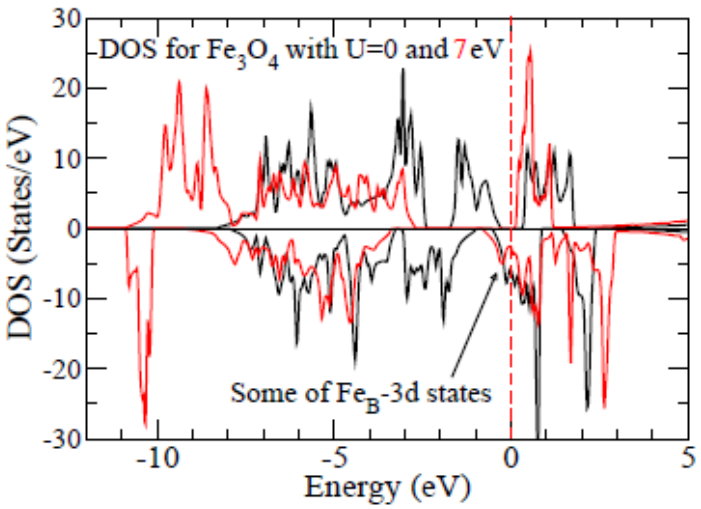

FIG. 2. Total DOS for (2Fe+2)[4Fe+3]O8 by GGA+U with U=0 (black) and U=7 eV (red).

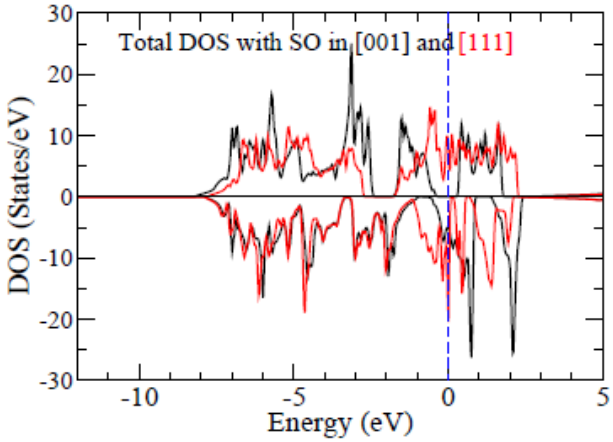

FIG. 3. Spin-Orbit Coupling in directions parallel to [001] and [111] directions for $(2Fe^{+2})[4Fe^{+3}]O_8$.

The DOS, not shown here, shows metallic behaviors for the four configurations, and the most stable one is $(2Fe^{+2})[Fe^{+2}\ 3Fe^{+3}]O_8$ which has a configuration in agreement with ref [18]. The recorded space groups of these configurations in column 2 of table 1 have been calculated by suppercell calculations as implemented in Wien2k code. The magnetic moment for $(2Fe^{+2})[Fe^{+2}\ 3Fe^{+3}]O_8$ is 3.37μB for A-site iron but 3.46μB and 1.55μB for the two types of iron in B-site. The total spin magnetic moment is 2.29μB per formula unit with energy 16477.70693Ry. Correlation has been done for such distribution by applying U=3 eV but thisdoes not destroy themetallic behavior, and no convergence occurs for U higher than 3 eV. D. J. Huang et.al have published measurements of spin and orbital magnetic moments of $FeFe_2O_4$ and magnetic circular dichroism [28]. These measurements have shown that $FeFe_2O_4$ has a non-integer spin moment and it has also exhibited a large unquenched orbital moment. D. J. Huang and others have indicated strong correlations and spin-orbit interaction of the 3d electrons resulting in the non-integer spin and large orbital moments of $FeFe_2O_4$ using the local density approximation including the Hubbard U method.

TABLE I. Different studied cation configurations for $FeFe_2O_4$ ferrite.

Structure	Space group	Energy [Ry]	μ_B
$(2Fe^{+2})[4Fe^{+3}]O_8$	Fd-3m	**-16477.87622176**	8
$(2Fe^{+2})[Fe^{+2}\ 3Fe^{+3}]O_8$	R-3m	**-16477.70692763**	2.28608
$(2Fe^{+2})[2Fe^{+2}\ 2Fe^{+3}]O_8$	Imma	-16477.66792778	1.00473
$(2Fe^{+3})[2Fe^{+2}\ 2Fe^{+3}]O_8$	Imma	-16477.68846099	9.03434
$(2Fe^{+2})[2Fe^{+3}\ 2Fe^{+3}]O_8$	Imma	-16477.68844899	9.04902

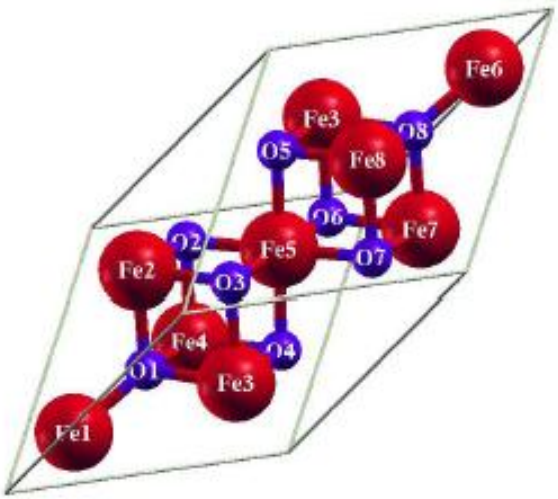

FIG. 4. The two spinel sublattices A- and B-sites in the primitive cell mode structure.

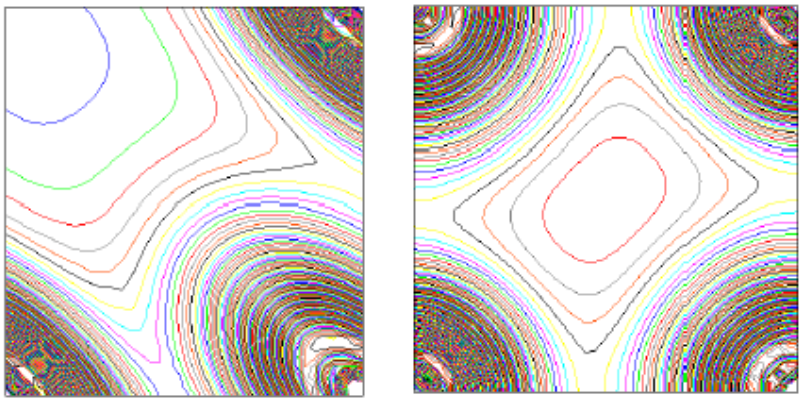

(a)site resolved for tetrahedral sublattice **(b)**site resolved for octahedral sublattice

FIG. 5. electron density in spin down-direction which shows bonding states for site resolved in tetrahedral sub lattice and antibonding states in octahedral sublattice for $(2Fe^{+2})[4Fe^{+3}]O_8$.

Regarding the above, the magnetic anisotropy within Spin-Orbit Coupling has been calculated in three different directions of the magnetization for $(2Fe^{+2})[4Fe^{+3}]O_8$. These directions have been assumed to be in parallel to the [100], [001] and [111] directions. A conductive behavior in both channel for the [111] direction is shown in figure 3. Whereas the half metallicityfor the [001] and [100]directionsareshown.

The direction [111] passes through the unsymmetrical crowded block formed by Fe2, 3, 4, 5 and O1, 2, 3, 4 as shown in figure 4. Hence the crystal field produced by the three iron atoms is expected to be high in [111] direction.Which in turn force some 3d states above the Fermi level. Detailed calculations for the bond lengths, A and B- sites dimensions shown in figure 4, have been carried out. As for A-site, the three edges of the face formed by Fe1, Fe2 and Fe3 have length 2.9748°A but all the other faces have edges with length 3.4883°A. Additionally, unequal distances have been observed among the oxygen atoms in B-site. Where the distance between O3!O5 and O3!O7 is 2.976°A but the distance between O3!O1, O3!O2 and O3!O4 is 2.8556°A. These deformations in A and B-sites urge us to believe that the magnetite should have a space group lower than 227. Unequal interatomic distances cause different spin behavior for Fe-3d and O-2p electrons. Additionally, narrow and wide interatomic distances cause high and low crystal field respectively. The high crystal field forces some states to pass Fermi level leading to half-metallicity of minority channels. Worthy mentioned, there are many states in which there are differences in sign of the wave functions on adjacent atomic nuclei see fig.1 in ref. [4]. Thus, the 3d and 2p wave functions change the sign along the different interatomic distances leading to a node in the wave function. This does not mean that the cation and anion cannot be bonded together.Yet; the wave function with a node is expected to contribute a weaker bonding than that without a node. This weak bonding or high energy case (antibonding state) in figure 5-b between O-2p and FeB-3d is the reason for the half metallicity produced by some 3d minority occupied states in B-site shown in figure 2. Whereas the strong bonding state or low energy case has been observed between O-2p and FeA-3d as shown in Figure 5-a. Where FeB is the B-site iron or Fe5 in figure 4 and FeA is the A-site iron or Fe1 in figure 4. The calculations show that the splitting of FeA-3d states is in agreement with the crystal field theory (CFT). Where, the tetrahedral crystal field splits the d-orbital into e_g with lower energy and t_{2g} with higher energy as shown in figure 6. As for the octahedral site, a nearly overlap between e_g and t_{2g} has been observed at Fermi level as shown in figure 6. Where a dispersion band in the vicinity of Fermi energy for minority channel is formed from t_{2g} and e_g states of FeB-3d. This in turn forms something like half-full band that occurs in metals. That half-full band is the reason for the half-metallicity of $FeFe_2O_4$. This band was observed experimentally byW.Wang in ref [31].

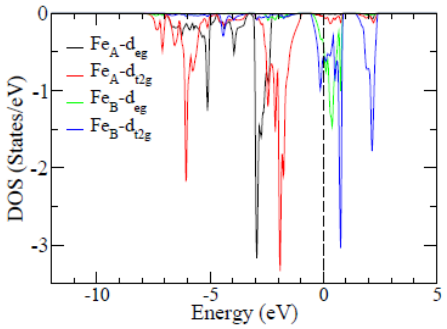

FIG. 6. The DOS for FeA-3d and FeB-3d with the labels of the molecular symmetry theory for $(2Fe^{+2})[4Fe^{+3}]O_8$.

Additionally, the octahedral crystal field does not produce e_g with energy higher than t_{2g} as expected by CFT for octahedral sublattice. That is because, the antibonding behavior in figure 5-b increases the energy of occupied state t_{2g} until it overlaps with e_g. As for the magnetic moment, the studied normal spinel structure contains two types of iron different by position and ionization. The calculated magnetic moments for these two types of iron are 3.42μB and 3.49μB for FeA and FeB respectively. The projected DOS in Fig 6 indicates that FeA in tetrahedral sites with the +2 state should have the electronic configuration $e3_g\ t3_{2g}$ predicting a magnetic moment of 4 μB. The case is different for FeB which has partially occupied and hybridized e_g and t_{2g} just down Fermi level with $t3_{2g}e_{2g}$ leading to 5μB. The hybridization or the little difference in energy showed in figure 6 for e_g and t_{2g} for FeB indicates that the pairing energy is higher than the energy difference between e_g and t_{2g}. Such strengthen of the previous unpaired electronic configurations for FeB and FeA causes high magnetic moment state for FeB. Additionally the excess of magnetic moment 4μB and 5μB than the calculated values 3.42μB and 3.49μB is due to the calculation mechanism which partitioning the unit cell into atomic spheres and an interstitial regions carrying a part of the moment.

IV. Summary And Conclusions

Ab initio calculations have been used to examine the electronic structure of $FeFe_2O_4$ spinel compound. Full optimizations for the oxygen position parameter and lattice constant have been carried out. To sum up, the reason for the half-metallicity of $FeFe_2O_4$ has been determined by the bond analysis of A- and B-sites and con-tour representation. FeB-3d electrons are localized forming antibonding states with ligands. This antibonding increases the FeB-3d electrons energy which forms dispersion band in the vicinity of Fermi energy for minority channel. This dispersion band includes the t_{2g} and e_g states of FeB-3d that overlap to each other at Fermi energy. This in turn forms something like half-full band that occurs in metals. That half-full band is the reason for the half-metallicity of $FeFe_2O_4$.

References

[1]. A. Zerr, G. Miehe, G. Serghiou, M. Schwarz, E. Kroke,R. Riedel, H. FueB, P. Kroll, and R. Boehler, Nature(London) 400, 340 (1999).
[2]. T. Sato, H. Yokoyama, K. Yamasawa, K. Toya,S. Kobayashi, and T. Minamisawa, Electrical Engineer-ing in Japan 135, 1 (2001).
[3]. A. P. Cracknell, Rep. Prog. Phys. 32, 633 (1969).
[4]. S. Soliman, A. Elfalaky, G. H. Fecher, and C. Felser,Physical Review B 83, 085205 (2011).
[5]. C. M. B. Henderson, J. M. Charnock, and D. A. Plant,Journal of Physics: CondensedMatter 19, 076214 (2007).
[6]. F. Burghart, W. Potzel, G. Kalvius, E. Schreier,G. Grosse, D. Noakes, W. Schafer, W. Kockelmann,S. Campbell, W. Kaczmarek, A. Martin, and K. M.Krause, Physica B 289, 286 (2000).
[7]. K. E. Sickafus and J. M. Wills, J. Am. Ceram. Soc. 82,3279 (1999).
[8]. I. Masahiko and U. Yutaka, Journal of Alloys and Com-pounds 383, 85 (2004).
[9]. D. I. Khomskii and T. Mizokawa, Cond-mat 1, 0407458(2004).
[10]. A. Szytula and L. Gondek, ActaPhysicaPolonica A 106,583 (2002).
[11]. J. Takaobushi, M. Ishikawa, S. Ueda, E. Ikenaga,J. Kim, M. Kobata, Y. Takeda, Y. Saitoh, M. Yabashi,Y. Nishino, D. Miwa, K. Tamasaku, T. Ishikawa,I. Satoh, H. Tanaka, K. Kobayashi, and T. Kawai, Physical Review B 76, 205108 (2007).
[12]. A. Hudson and H. Whitfield, Molecular Physics 12, 165(1967).
[13]. V. Sepelak, U. Steinike, D. C. Uecker, and S.Wi, Journalof Solid State Chemistry 135, 52 (1998).
[14]. S. Sakurai, S. Sasaki, M. Okube, H. Ohara, and T. Toy-oda, Physica B 403, 3589 (2008).
[15]. K. Kamazawa, Y. Tsunoda, H. Kadowaki, and K. Kohn,Physical Review B 68, 024412 (Jul 2003).
[16]. F. A.G., V. Raposo, L. Torres, and J. Iniguez, PhysicalReview B 59, 9447 (1999).
[17]. S. Z., W. M. Temmerman, D. Kdderitzsch, A. Svane, andL. Petit, Physical Review B 74, 174431 (2006).
[18]. I. Leonov, A. Yaresko, V. Antonov, M. Korotin, andV. Anisimov, Phys Rev Lett. 93, 146404 (2004).
[19]. K. Kamazawa, Y. Tsunoda, K. Odaka, and K. Kohn,Journal of Physics and Chemistry of Solids 60, 1261(1999).
[20]. D. Levy, R. Giustetto, and A. Hoser, Physics and Chem-istry of Minerals 39, 169 (2011).
[21]. P. Blaha, K. Schwarz, P. Sorantin, and S. B. Tricky, Com-put. Phys. Commn. 59, 399 (1990).
[22]. P. Blaha, K. Schwarz, M. G. K. H, D. Kvasnicka, andJ. Luitz, WIEN2k, An Augmented Plane Wave + Lo-cal Orbitals Program for Calculating Crystal PropertiesKarlheinz Schwarz, Techn. Universitat Wien, wienAus-tria(2001).
[23]. John, P. Perdew, B. Kieron, and E. Matthias, PhysicalReview letters 77, 3865 (1996).
[24]. J. Charnock, C. D. Garner, R. A. D. Pattrick, and D. J.Vaughan, American Mineralogist 75, 247 (1990).
[25]. M. Penicaud, B. Siberchicot, C. B. Sommers, and J. Ki-ibler, Journal of Magnetism and Magnetic Materials 103,212 (1992).
[26]. A. Yanase and K.Siratori, J. Phys. Soc. Jpn. 53, 312(1984).
[27]. Z. Zhang and S. Satpathy, Physical Review B 44, 13319(1991).
[28]. D. J. Huang, C. F. Chang, H.-T. Jeng, G. Y. Guo, H.-J.Lin, W. B.Wu, H. C. Ku, A. Fujimori, Y. Takahashi, andC. T. Chen, Physical Review Letters 93, 077204 (2004).
[29]. D. J. Singh, M. Gupta, and R. Gupta, Physical ReviewB 63, 205102 (2001).
[30]. M. Fonin, R. Pentcheva, Y. S. Dedkov, M. Sperlich, D. V.Vyalikh, M. Scheffler, U. Rdiger, and G. Gntherodt,Physical Review B 72, 104436 (2005).
[31]. W. Wang, J. Mariot, M. C. Richter, O. Heckmann,W. Ndiaye, P. D. Padova, A. Taleb-Ibrahimi, P. L. Fevre,F. Bertran, F. ondino, E. Magnano, J. Krempasky,P. Blaha, C. Cacho, F. Parmigiani, and K. Hricovini,Physical Review B 87, 085118 (2013).